Journal of Hydroscience and Hydraulic Engineering
Vol. 20, No.1 May, 2002, 113-125

3D NUMERICAL SIMULATION OF FLOW AND LOCAL SCOUR AROUND A CYLINDRICAL PIER

by

N. NAGATA (Deceased in December 2000), T. HOSODA

Department of Civil Engineering, Kyoto University,
Yoshida, Sakyo-Ku, Kyoto 606-8501, Japan

T. NAKATO

IIHR, Department of Civil and Environmental Engineering, The University of Iowa,
Iowa City, IA 52242, U.S.A.

and

Y. MURAMOTO

Professor Emeritus of Kyoto University, Osaka College of Technology,
1-9-27, Tenma, Kita-Ku, Osaka 530-0043, Japan

SYNOPSIS

Prediction of damage due to local scour around a bridge pier is of crucial importance to bridge safety. However, it is extremely difficult to solve analytically complex flow associated with local bed deformation surrounding the pier. This paper describes the development of a numerical model in simulating flow and bed deformation around a cylindrical pier. The flow was calculated using 3D Reynolds-averaged Navier-Stokes equations closed with a nonlinear $k-\varepsilon$ turbulence model. A moving boundary-fitted coordinate system was used to simulate the unsteady flow field bounded by movable bed surface and free water surface. The effect of non-equilibrium sediment transport was introduced in the bed-deformation model by coupling the momentum equation of sediment with stochastic models for sediment pick-up and deposition. The model proposed in this study was tested against laboratory data for verification. It was found that the model can reproduce the flow and local scour geometry with reasonable accuracy.

INTRODUCTION

In view of bridge safety during floods, numerous studies concerning local scour around a bridge pier have been conducted to clarify the flow structures and sediment transport mechanism, and to estimate the maximum scour depth. Extensive investigations based on fundamental physical models have revealed complex three dimensional flow structures around the bridge pier and the effect of hydraulic parameters on local scour patterns. Investigations of this subject were reviewed by Breusers et al. (1977) and Dey (1997).

Several numerical studies have been conducted in recent years to calculate not only scour depth but also scour geometry, such as: (1) flow around a cylindrical pier (Richardson and Panchang (1998); and (2) flow and bed variations around a cylindrical pier (Olsen and Melaaen (1993), Fukuoka et al. (1994), Olsen and Kjellesvig (1998), Roulund et al. (1998)).

Richardson and Panchang calculated flow structures around a cylindrical pier with a fixed bed scour hole by means of the commercial software, FLOW 3-D. However, in their numerical results, the horseshoe vortex and reversal flow near the bed in the scour hole were not reproduced well. Olsen and Melaaen, and Olsen and Kjellesvig conducted the computations of flow using the standard k- ε turbulence model and of bed deformation due to suspended-load transport. Since the calculated geometry of scour hole was not compared with the experimental one, we could not ascertain the applicability and accuracy of their numerical model.

Fukuoka et al. combined 3-D flow computation with both an empirical eddy viscosity equation and the assumption of hydrostatic pressure, and a bed deformation model including nonequilibrium sediment transport processes. They divided the downstream area of a bridge pier into three areas: (1) the region where nonequilibrium sediment transport is dominant because near-bed flow and bed configuration rapidly change due to the presence of the pier and scour hole, (2) the region where local equilibrium of sediment transport can be assumed, and (3) the transitional region. However, the method for discriminating each region under various hydraulic conditions was not validated. Roulund, et al.(1998) also carried out calculations of flow and bed deformation processes. The conventional method using a sediment continuity equation and a bed-load transport equation in an equilibrium state was used for calculating bed deformation with the software for 3-D flow calculation, EllipSys3D. Although it was shown that the computed flow patterns are in good agreement with the observed results to some extent, the computed results of scour hole geometry behind a pier, where nonequilibrium sediment transport is dominant, were not satisfactory.

In view of these arguments, we developed a numerical model in simulating overall characteristics of flow and bed deformation around a cylindrical pier, combining a fully 3D flow model with a nonlinear $k-\varepsilon$ turbulence model and a nonequilibrium sediment transport model in a moving boundary fitted coordinate system. Model verification was also conducted by comparing the computed results with previous laboratory tests.

FUNDAMENTAL EQUATIONS TO CALCULATE 3D FLOW STRUCTURES

The writers have analyzed unsteady open channel flows and river channel processes with bank erosion by the depth-averaged 2D numerical model that was developed using moving boundary-fitted coordinates to conform numerical grids to both shifting side banks (Hosoda et al. (1996) and Nagata et al. (2000)). This analysis revealed that a moving grid system is an effective tool for simulating the unsteady flow field with temporal changes in channel geometry. Ushijima et al.(1998) also applied a numerical model using moving boundary-fitted coordinates to local scour due to cooling-water jets discharged from power plants. In this study, to calculate the flow with water and bed surfaces varying with time, a 3D flow model using moving a boundary-fitted coordinate system was adopted.

The fully three dimensional Reynolds-averaged Navier-Stokes (RANS) equation and the continuity equation expressed in a moving boundary-fitted coordinates are as follows:

- Momentum

$$\frac{\partial}{\partial t}\left(\frac{U^i}{J}\right)+\frac{\partial}{\partial \xi^j}\left(\frac{(U^j-U_G^j)U^i}{J}\right)-\frac{\left(U^j-U_G^j\right)\mathbf{u}}{J}\cdot\frac{\partial}{\partial \xi^j}\left(\nabla\xi^i\right)-\frac{\mathbf{u}}{J}\cdot\frac{\partial}{\partial t}\left(\nabla\xi^i\right)$$
$$=-\frac{g^{ij}}{\rho J}\frac{\partial p}{\partial \xi^j}+\frac{\mathbf{f}}{J}\cdot\nabla\xi^i+\frac{1}{J}\frac{\partial \xi^j}{\partial x^m}\frac{\partial \xi^i}{\partial x^l}\frac{\partial}{\partial \xi^j}\left(\tau^{lm}-\overline{u'^l u'^m}\right) \tag{1}$$

- Continuity

$$\frac{\partial}{\partial \xi^j}\left(\frac{U^j}{J}\right)=0 \tag{2}$$

in which

$$\nabla\equiv\left(\frac{\partial}{\partial x^1},\ \frac{\partial}{\partial x^2},\ \frac{\partial}{\partial x^3}\right),\quad g^{ij}\equiv\nabla\xi^i\cdot\nabla\xi^j \tag{3a, b}$$

$$U^i\equiv(\partial\xi^i/\partial x^j)\ u^j,\quad U_G^i\equiv(\partial\xi^i/\partial x^j)\ u^j{}_G \tag{3c, d}$$

$$\tau^{ij}=\nu\left(\frac{\partial \xi^m}{\partial x^j}\frac{\partial u^i}{\partial \xi^m}+\frac{\partial \xi^m}{\partial x^i}\frac{\partial u^j}{\partial \xi^m}\right) \tag{3e}$$

where t = time; (x^1,x^2,x^3) = Cartesian coordinates (x^3 denotes the vertical coordinate); (ξ^1,ξ^2,ξ^3) = boundary-fitted coordinates; ρ = fluid density; ν = kinematic viscosity; p = pressure; J = Jacobian of transformation; g^{ij} = contravariant metric tensors; U^i = contravariant components of velocity; U_G^i = contravariant components of grid velocity; $\mathbf{u}$ = velocity vector ($\mathbf{u}=(u^1,u^2,u^3)$); u^i = velocity components in Cartesian coordinates; u_G^i = grid velocity components in Cartesian coordinates; $\mathbf{f}$ = gravity acceleration vector ($\mathbf{f}=(0,0,-g)$); g = magnitude of gravity acceleration; τ^{ij} = viscous stress tensors; and $-\overline{u'^i u'^j}$ = Reynolds stress tensors in Cartesian coordinates.

Since 3D flow structures are dominant around a bridge pier, a nonlinear $k-\varepsilon$ model with empirical functions by Hosoda et al. (1999) and Kimura and Hosoda (1999, 2000) were used to calculate Reynolds stress tensors .

The Reynolds stress tensors are expressed by the following expressions (Yoshizawa 1984):

$$-\overline{u'^i u'^j} = D_t\left(\frac{\partial \xi^m}{\partial x^j}\frac{\partial u^i}{\partial \xi^m}+\frac{\partial \xi^m}{\partial x^i}\frac{\partial u^j}{\partial \xi^m}\right)-\frac{2}{3}k\delta^{ij} \quad -\frac{k}{\varepsilon}D_t\sum_{\beta=1}^{3}C_\beta\left(S_\beta{}^{ij}-\frac{1}{3}S_\beta{}^{\alpha\alpha}\delta^{ij}\right) \tag{4}$$

in which

$$S_1^{ij}=\frac{\partial u^i}{\partial x^r}\frac{\partial u^j}{\partial x^r}\ , \quad S_2^{ij}=\frac{1}{2}\left(\frac{\partial u^r}{\partial x^i}\frac{\partial u^j}{\partial x^r}+\frac{\partial u^r}{\partial x^j}\frac{\partial u^i}{\partial x^r}\right), \quad S_3^{ij}=\frac{\partial u^r}{\partial x^i}\frac{\partial u^r}{\partial x^j} \tag{5a, b, c}$$

(4) and (5a,b,c) are equivalent to the expressions by Gatski and Speziale (1993). The eddy viscosity coefficient D_t and other coefficients C_μ, C_1, C_2, C_3 are formulated as follows:

$$D_t=C_\mu\frac{k^2}{\varepsilon}, \quad C_\mu=\min\left[0.09,\ \frac{0.3}{1+0.09M^2}\right] \tag{6a, b}$$

$$C_1=\frac{0.4}{1+0.01M^2}, \quad C_2=0, \quad C_3=\frac{-0.13}{1+0.01M^2} \tag{6c, d, e}$$

The parameter M in (6) is estimated using the strain parameter S and rotation parameter Ω as follows:

$$M=\max(S,\Omega) \tag{7}$$

$$S=\frac{k}{\varepsilon}\sqrt{\frac{1}{2}\left(\frac{\partial u^i}{\partial x^j}+\frac{\partial u^j}{\partial x^i}\right)^2}\ , \quad \Omega=\frac{k}{\varepsilon}\sqrt{\frac{1}{2}\left(\frac{\partial u^i}{\partial x^j}-\frac{\partial u^j}{\partial x^i}\right)^2} \tag{8a, b}$$

The turbulent kinetic energy k and its rate of dissipation ε, which appear in (4), (6a), and (8a,b), are obtained by using the following transport equations expressed in moving boundary coordinates:

$$\frac{\partial}{\partial t}\left(\frac{k}{J}\right)+\frac{\partial}{\partial \xi^j}\left(\frac{\left(U^j-U_G^j\right)k}{J}\right)=\frac{-\overline{u'^i u'^j}}{J}\frac{\partial \xi^l}{\partial x^j}\frac{\partial u^i}{\partial \xi^l}-\frac{\varepsilon}{J}+\frac{\partial}{\partial \xi^l}\left(\left(\nu+\frac{D_t}{\sigma_k}\right)\frac{g^{lm}}{J}\frac{\partial k}{\partial \xi^m}\right) \tag{9}$$

$$\frac{\partial}{\partial t}\left(\frac{\varepsilon}{J}\right)+\frac{\partial}{\partial \xi^j}\left(\frac{\left(U^j-U_G^j\right)\varepsilon}{J}\right)=C_{\varepsilon 1}\frac{\varepsilon}{k}\frac{\left(-\overline{u'^i u'^j}\right)}{J}\frac{\partial \xi^l}{\partial x^j}\frac{\partial u^i}{\partial \xi^l}-\frac{C_{\varepsilon 2}}{J}\frac{\varepsilon^2}{k}+\frac{\partial}{\partial \xi^l}\left(\left(\nu+\frac{D_t}{\sigma_\varepsilon}\right)\frac{g^{lm}}{J}\frac{\partial k}{\partial \xi^m}\right) \tag{10}$$

Model constants in (9) and (10) used in this calculation were $\sigma_k=1.0$, $\sigma_\varepsilon=1.3$, $C_{\varepsilon 1}=1.44$, and $C_{\varepsilon 2}=1.92$, respectively.

NUMERICAL MODEL FOR BED DEFORMATION

In the case of a bridge pier and the associated scour hole, the near-bed flow and the bed slope, which have significant influence on sediment movement, change rapidly around the structure. Therefore, the assumption of equilibrium sediment transport is questionable in this simulation. In view of this, we introduced the effect of nonequilibrium transport of sediment by calculating (1) the volume of sediment pickup; (2) traces of sediment motion; and (3) sediment deposition volume. The volume of sediment pickup and deposition can be obtained by employing a stochastic model of sediment motion. Sediment movement was calculated by a momentum equation of sediment particles. From the pickup and deposition volumes, the temporal changes in the bed elevation were obtained.

The volume of sediment pickup per unit time from a numerical mesh on a bed, V_p, is given by

$$V_p = \frac{A_3 d}{A_2} p_s S_p \tag{11}$$

where p_s = pickup rate; d = diameter of bed material; A_2, A_3 = shape coefficients of sand grain for two- and three-dimensional geometrical properties, respectively (= $\pi/4$, $\pi/6$); and S_p = area of the bed surface mesh projected onto the horizontal ($x^1 - x^2$) plane. The pickup rate, p_s, is evaluated from the following equation proposed by Nakagawa et al. (1986), which includes the effect of the local bed slope on sediment motion:

$$p_s \sqrt{\frac{d}{(\sigma/\rho - 1)g}} = F_0 G_* \tau_* \left(1 - \frac{k_p \Phi \tau_{*c}}{\tau_*}\right)^{m_p} \tag{12}$$

$$G_* = \frac{\cos\psi + k_L \mu_s}{1 + k_L \mu_s}, \quad \Phi = \frac{\mu_s \cos\theta_b - \sin\theta_b \cos\alpha}{\cos\psi + k_L \mu_s} \frac{1 + k_L \mu_s}{\mu_s} \tag{13a,b}$$

where τ_* = magnitude of dimensionless tractive stress vector; τ_{*c} = magnitude of dimensionless critical tractive stress vector; G_* = coefficient of deviation between near-bed velocity vector and sediment movement direction; Φ = coefficient of side bank slope; σ = density of sediment; μ_s = static friction factor (= 0.7); k_L = ratio between drag and lift forces (= 0.85); θ_b = local bed slope angle, ψ = angle between near-bed velocity vector and sediment movement direction; α = angle between the direction of maximum local bed slope and the sediment movement direction; and F_0, k_p, and m_p = constants (= 0.03, 0.7, and 3, respectively).

To formulate sediment movement, we first introduce the unit vectors $\mathbf{p}_{b1}$ and $\mathbf{p}_{b2}$, which are parallel to a local bed surface, on the ($x^1 - x^3$) and the ($x^2 - x^3$) planes, respectively.

$$\mathbf{p}_{b1} = \begin{pmatrix} \cos\theta_{b1} \\ 0 \\ \sin\theta_{b1} \end{pmatrix}, \quad \mathbf{p}_{b2} = \begin{pmatrix} 0 \\ \cos\theta_{b2} \\ \sin\theta_{b2} \end{pmatrix} \tag{15a, b}$$

where θ_{b1}, θ_{b2} = angles of bed inclination in the x^1 and x^2 directions, respectively. The momentum equation of sediment in the $\mathbf{p}_{bi}$ (i =1, 2) direction is

$$\rho\left(\frac{\sigma}{\rho} + C_m\right) A_3 d^3 \frac{\partial u_{sed\,i}}{\partial t} = D_i + W_i - F_i \tag{16}$$

$$D_1 = D\frac{u_{b1} - u_{sed1}}{\sqrt{(u_{bi} - u_{sed\,i})^2}}, \quad D_2 = D\frac{u_{b2} - u_{sed\,2}}{\sqrt{(u_{bi} - u_{sed\,i})^2}} \tag{17a, b}$$

$$W_1 = -W\frac{\sin\theta_{b1}\cos^2\theta_{b2}}{\sin^2\theta_p}, \quad W_2 = -W\frac{\sin\theta_{b2}\cos^2\theta_{b1}}{\sin^2\theta_p} \tag{17c, d}$$

$$F_1 = F\frac{u_{sed1}}{\sqrt{u_{sedi}^2}}, \quad F_2 = F\frac{u_{sed\,2}}{\sqrt{u_{sedi}^2}} \tag{17e, f}$$

$$D = \frac{C_D \rho}{2}(u_{bi} - u_{sedi})^2 A_2 d^2, \quad W = (\sigma - \rho) g A_3 d^3, \quad F = \mu_k\left(W\frac{\cos\theta_{b1}\cos\theta_{b2}}{\sin\theta_p} - k_L D\right) \tag{18a,b,c}$$

where C_m = coefficient of added mass; $u_{sed\,i}$ = sediment movement velocity; D = fluid drag force on a sediment particle; W = submerged weight of a sediment particle; F = friction force between sediment particles and the bed; u_{bi} = near-bed fluid velocity (at the distance of $k_d d$ from the bed); k_d = constant (= 0.7); C_D = drag coefficient (= 0.4); μ_k = kinetic friction factor (= 0.35); θ_p = angle between $\mathbf{p}_{b1}$ and $\mathbf{p}_{b2}$;

and subscript i denotes its components in the $\mathbf{p}_{bi}$ direction.

By using the vector of sediment movement velocity $\mathbf{u}_{sed}$ obtained by (16), the position vector of sediment after n-th step from sediment pickup, $\mathbf{p}_{sed(n)}$, and the distance of sediment movement, $s_{(n)}$, can be calculated by

$$\mathbf{p}_{sed(n)} = \mathbf{p}_{sed(n-1)} + \Delta t \cdot \mathbf{u}_{sed} \tag{19}$$

$$s_{(n)} = \sum \Delta t \left| \mathbf{u}_{sed} \right| \tag{20}$$

The deposition volume $V_{d(j,n)}$ of the sediment moving from point j at the time it reaches the position of $\mathbf{p}_{sed(n)}$ can be obtained by

$$V_{d(j,n)} = V_{p(j)} f_s(s_{(n)}) \left| \mathbf{u}_{sed(n)} \right| \Delta t \tag{21}$$

$$f_s(s_{(n)}) = \frac{1}{\lambda} \exp\left(-\frac{s_{(n)}}{\lambda} \right) \tag{22}$$

where $V_{p(j)}$ = volume of sediment pickup at point j; $f_s(s_{(n)})$ = probability density function of step length; and λ = average step length. In order to estimate λ, the following equation proposed by Einstein (1950) was adopted.

$$\lambda = \lambda_0 d \Big/ \int_{-B_*/\tau_*-1/\eta_0}^{B_*/\tau_*-1/\eta_0} \frac{1}{\sqrt{2\pi}} \exp\left(-\frac{r^2}{2} \right) dr \tag{23}$$

where η_0 = coefficient of variation of the lift force (= 0.5); and B_*, λ_0 = constants (0.156 and 100, respectively).

By using the pickup and deposition volumes calculated by (11) and (21), temporal changes in bed elevation can be obtained by

$$\frac{\partial z_b}{\partial t} = \frac{A_1 A_2}{A_3} \frac{(V_d - V_p)}{S_d} \tag{24}$$

where z_b = bed elevation; A_1 = shape coefficient of sand grain for one-dimensional geometrical properties (= 1.0); and S_d = area of the bed surface mesh projected onto the horizontal ($x^1 - x^2$) plane where sediment deposition takes place. In Eq.(24), V_d at a cell surrounded by four grid lines is calculated by adding $V_{d(j,n)}$ with respect to j over a whole flow domain at a time step.

CALCULATED RESULTS AND COMPARISONS WITH LABORATORY EXPERIMENTS

Test Cases

In order to validate the present model, we used it in laboratory experiments of flow and bed deformation around the bridge pier. The conditions of test cases for the bridge pier (Case 1 with a fixed bed and 2 with a movable bed) are summarized in Table 1. Re(h) and Re(D) appearing in Table 1 are the Reynolds number estimated by using the flow depth in the undisturbed region and the pier diameter as the characteristic length scale, respectively.

Results

Calculations under the conditions of Case 1 and 2 were carried out in order to validate the applicability of the numerical model to flow and bed variations around the bridge pier. These cases corresponded to the laboratory experiments conducted by Melville (1975), Melville and Raudkivi (1977) and Dey et al. (1995). Richardson and Panchang (1998) also applied their proposed models for verification. Their experiments were conducted in a

Table 1. Test Cases

	Discharge (m^3/s)	Channel width (m)	Bed slope	Flow depth (m)	Mean approach velocity (m/s)	Froude Number	Re(h)	Re(D)	Structure	Bed
Case 1	0.01712	0.456	1/10000	0.15	0.250	0.21	37544	12715	Circular pier	Fixed bed
Case 2	0.01712	0.456	1/10000	0.15	0.250	0.21	37544	12715	Circular pier	Movable bed

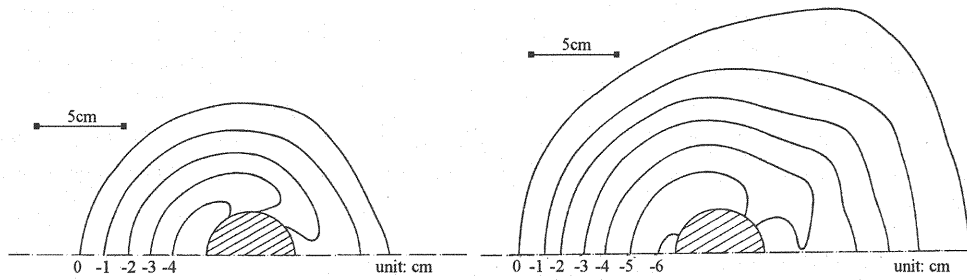

(a) Intermediate Stage (b) Equilibrium Stage

Fig. 1 Observed Bed Contours (Melville 1975)

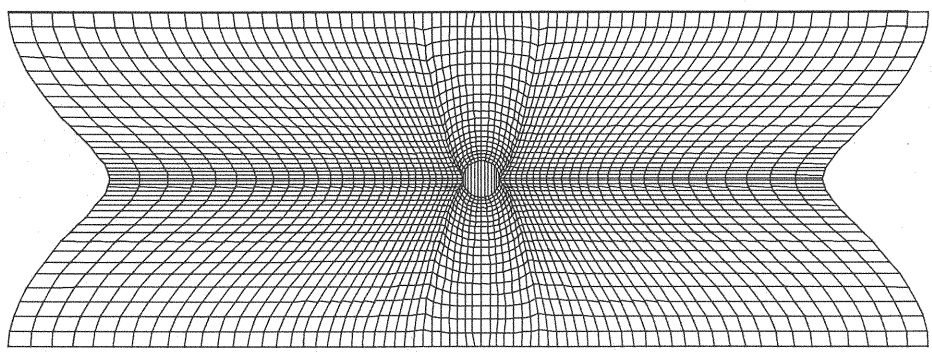

Fig. 2 Numerical Grid Around Cylindrical Pier in x-y Plane

19-m long and 45.6-cm wide flume. A cylinder with a 5.08-cm diameter was used as a bridge pier model. The bed material was a relatively uniform-sized sand with a median grain size of 0.385 mm. In order to clarify the flow structure in the scour hole region, flow measurements were taken by using concrete replicas of the scour holes, which were observed in the experiment with a movable bed in the intermediate (t = 30 min) and the equilibrium (t = 150 min) stages. Fig. 1 shows the scour hole topographies in both stages. The detailed description of the experiment is presented by Melville (1975) and Melville and Raudkivi (1977).

In Case 1, numerical analyses were performed to investigate the model applicability to the flow around a pier with scour hole using the scour geometry shown in Fig. 1 in which the fixed bed was used as a computational flow domain. Fig. 2 shows the numerical grid surrounding the cylindrical pier utilized in simulating Case 1. The numerical method, conditions of flow calculations and model performances by using a nonlinear $k-\varepsilon$ model are described in the studies by Hosoda, et al. (1999) and Kimura and Hosoda (1999, 2000)

Figs. 3 and 4 show velocity vectors and contours of their magnitudes that were normalized by the mean approach flow velocity (0.25 m/s) in a plane of symmetry upstream from the cylinder, respectively. The observed contours shown in Fig.4 (a, b) were based on the data measured at an interval of about 1cm. However, the measurement interval was too coarse in comparison with the scour hole scale to draw accurate contours, especially near the pier wall. Therefore, we limited the investigation to qualitative comparisons.

In the experimental results, a vertically downward flow in front of the circular pier and a rotating flow creating a horseshoe vortex near the bed were observed (see Fig. 3 (b, d)). A downward flow directed onto the bed induced a large velocity component near the bed, which distorted velocity contours in the vicinity of the circular pier as shown in Fig. 4 (a,b). These trends were captured fairly well by the numerical current simulation (Fig.4 (c, d)). The theoretical model proposed by Dey et al. (1995), in which the velocity components were determined so as to fit the experimental velocity profiles as well as to satisfy the continuity equation, did not express the shape of velocity contours with reasonable accuracy. In the numerical results obtained by Richardson and Panchang (1998), the vortical flow and the reversed flow near the bed were not clearly identified and the unique feature of high velocity isovel contours penetrating down to the scour hole was not reproduced. These results provide strong evidence of the advantage of the present model. Fig. 5 shows the observed and computed streamlines 2 mm from the bed. It is seen that the observed streamlines starting from the vicinity of the cylinder were directed away from the cylinder and met the streamlines of approaching flow along the separation line. The region where the reversed flows were observed in the equilibrium stage became larger compared with that of the intermediate stage. The numerical model reproduced the experimental results quite accurately.

In Case 2, the numerical simulation was performed for an initially flat fine-sand bed which corresponded to the experimental condition of the movable bed. Fig. 6 shows the computed topography of the scour hole in the equilibrium stage. Under the hydraulic condition of Case 2 shown in Table 1, the bed shear stress in the undisturbed region was slightly smaller than the critical bed shear stress for the bed material used in this case.

Because the local bed slope needed for calculation of pick-up rate was estimated by using bed elevations of neighboring numerical meshes, the pick-up rate on the mesh, including the edge of the scour hole, was influenced by the steep scour hole slope. As a result, bed scouring occurred gradually near the edge of the scour hole. This made the edge smooth in spite of the fact that the actual edge of the scour hole was sharp. For this reason, the "0" contour of the bed elevation shown in Fig. 6 shifted further away from the scour hole as compared with the experimental result shown in Fig. 1. Aside from this discrepancy, the overall scour geometry was reproduced reasonably well in the present model in comparison with the experimental results shown in Fig. 1. The computed shape of the scour hole is quite similar to the typical scour hole geometry around the circular pier observed by Yanmaz and Alt1nbilek (1991).

CONCLUSIONS

The numerical model in simulating flow and bed changes around the bridge pier was developed. The fully three-dimensional URANS equation with the nonlinear $k-\varepsilon$ turbulence model was adopted because of the strong three-dimensional flow which is characterized by the downward flow upstream from the pier and the horseshoe vortex near the bed. To simulate the unsteady flow with temporal changes in flow and bed surface, a moving boundary-fitted coordinate system was employed. Because the nonequilibrium transport of sediment was dominant around the pier, the effect of nonequilibrium sediment transport was introduced in the bed deformation model by coupling the stochastic model of sediment pickup and the momentum equation of sediment particles for deposition.

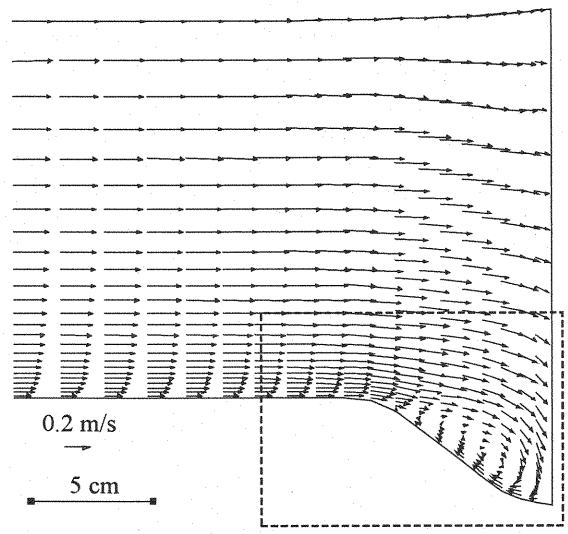

(a) Cal. (Intermediate Stage)

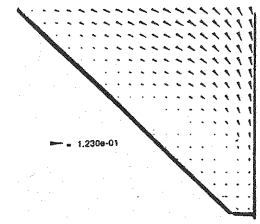

Cal. (Richardson and Panchang, 1998)

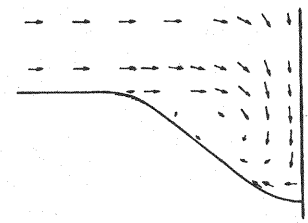

(b) Exp. (Intermediate Stage)

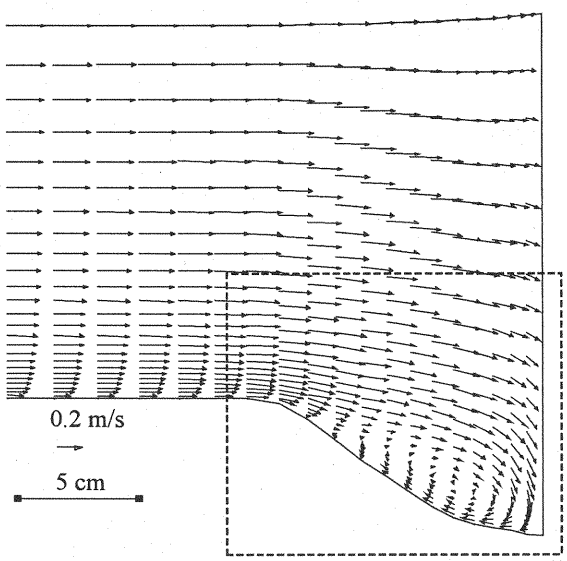

(c) Cal. (Equilibrium Stage)

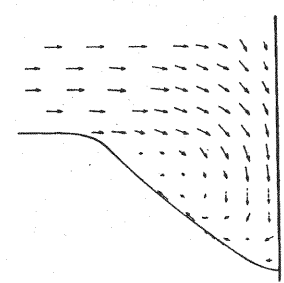

(d) Exp. (Equilibrium Stage)

Fig. 3 Velocity Vectors in Plane of Symmetry ahead of Circular Pier (Case 1): (a) Calculated Result in Intermediate Stage; (b) Observed Results in Intermediate Stage (Melville 1975); (c) Calculated Result in Equilibrium Stage; (d) Observed Results in Equilibrium Stage (Melville 1975)

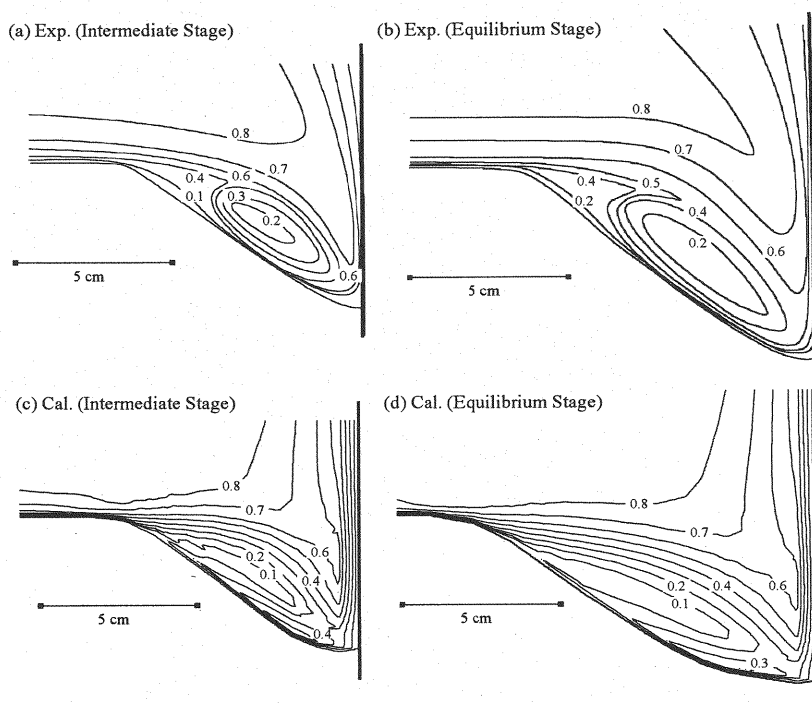

Fig. 4 Comparisons of isovels in plane of symmetry in Case 1

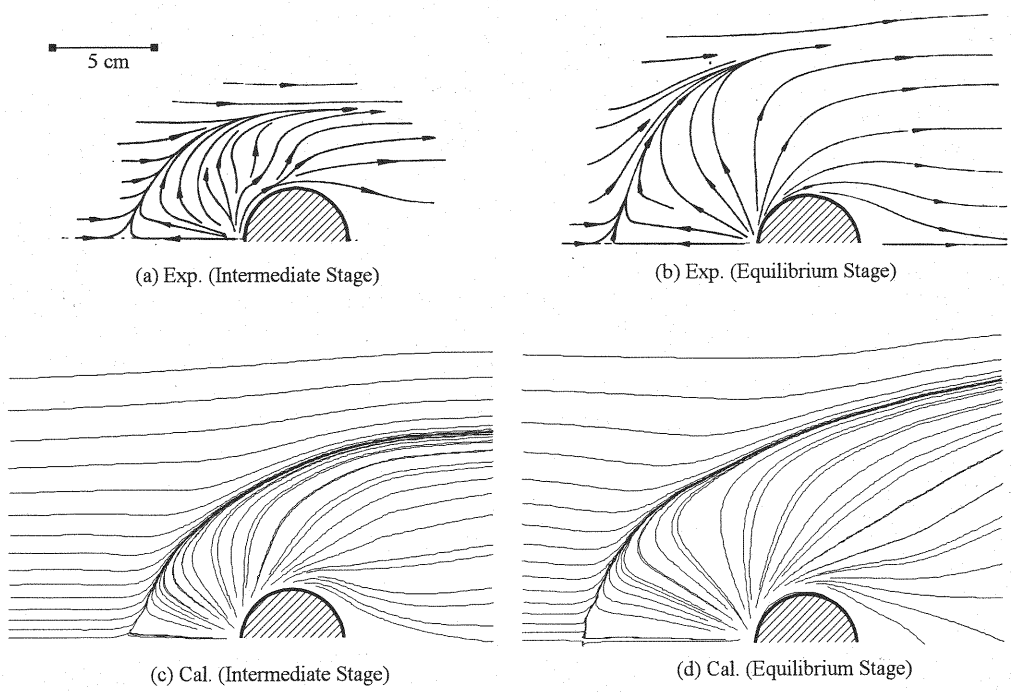

Fig. 5 Streamlines at 2 mm from Bed (Case 1)

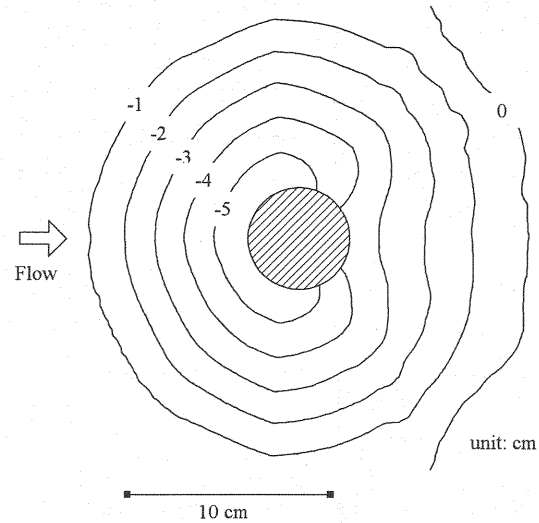

Fig. 6 Calculated Bed Contours around Circular Pier (Case 2)

The proposed model was applied to the existing laboratory data. It was pointed out that the present numerical model was found to reproduce flow and scour hole geometry around the pier with a sufficient accuracy.

Further studies are needed in order to clarify the sensitivity of the coefficients appearing in the bed deformation model. In this study, those coefficients were determined according to the previous study.

ACKNOWLEDGEMENTS

The main part of this study was conducted while the first writer was at Iowa Institute of Hydraulic Research (IIHR) as a visiting scholar financially supported by the Ministry of Education of Japan. The numerical simulations were carried out on a computer provided by IIHR. We appreciate the assistance of the IIHR staff members who provided a suitable research environment to make this study possible.

REFERENCES

Breusers, H. N. C., Nicolet, G., and Shen, H. W. (1977). "Local scour around cylindrical piers." *J. Hydr. Res.*, Delft, The Netherlands, 15(3), 211-252.

Dey, S. (1997). "Local scour at piers, Part I: A review of developments of research." *Int. J. Sediment Res.*, Beijing, China, 12 (2), 23-46.

Dey, S., Bose, S. K., and Sastry, G. L. N. (1995). "Clear water scour at circular piers: a model." *J. Hydr. Engrg.*, ASCE, 121(12), 869-876.

Einstein, H. A. (1950). "The bed load function for sediment transportation in open channel flows." Technical Bulletin, No.1026, U.S. Department of Agriculture, Soil Conservation Service.

Fukuoka, S., Tomita, K. Hotta, T. and Miyagawa, T. (1994). "Practical numerical simulation of local scour around a bridge pier. " *J. Hydr., Coast. and Envir. Engrg.*, JSCE, 497(2-28), 71-79 (in Japanese).

Gatski, T. B., and Speziale, C. G. (1993). "On explicit algebraic stress models for complex turbulent flows." *J. Fluid Mech.*, Cambridge, U.K.,254, 59-78.

Hosoda, T., Nagata, N. and Muramoto, Y.(1996). "Numerical analysis of unsteady open channel flows by means of moving boundary fitted coordinate system", *J. Hydr., Coast. and Envir. Engrg.*, JSCE, 533(2-34), 267-272 (in Japanese)..

Hosoda, T., Sakurai,T., Kimura,I. and Muramoto, Y.(1999). "3-D computations of compound open channel

flows with horizontal vortices and secondary currents by using non-linear k- ε model.", *J. Hydrsci. Hydr. Engrg.*, JSCE, 17(2), 87-96.

Kimura, I., and Hosoda, T. (1999). "3-D unsteady flow structures around rectangular column in open channels by means of non-linear $k-\varepsilon$ model." *Proc. 1st Int. Symp. on Turbulence and Shear Flow Phenomena,* Santa Barbara, California, 1001-1006.

Kimura, I. and Hosoda, T.(2000)."Numerical simulation of flows around a surface-mounted cube by means of a non-linear $k-\varepsilon$ model." *CD-Proc. of 7th International Symposium on Flow Visualization*, Edinburgh, Paper No.388.

Melville, B. W. (1975). "Local scour at bridge site." *Rep. No. 117*, School of Engrg., The Univ. of Auckland, New Zealand.

Melville, B. W., and Raudkivi, A. J. (1977). "Flow characteristics in local scour at bridge piers." *J. Hydr. Res.*, Delft, The Netherlands, 15(4), 373-380.

Nakagawa, H., Tsujimoto, T., and Murakami, S. (1986). "Non-equilibrium bed load transport along side slope of an alluvial stream", *Proc., 3rd Int. Symp. on River Sedimentation*, Jackson, Mississippi, 885-893.

Nagata, N., Hosoda, T., and Muramoto, Y. (2000). "Numerical analysis of river channel processes with bank erosion." *J. Hydr. Engrg.*, ASCE, 126(4), 243-252.

Olsen, N. R. B., and Kjellesvig, H. M. K. (1998). "Three-dimensional numerical flow modeling for estimation of maximum local scour depth." *J. Hydr. Res.*, Delft, The Netherlands, 36(4), 579-590.

Olsen, N. R. B., and Melaaen, M. C. (1993). "Three-dimensional calculation of scour around cylinders." *J. Hydr. Engrg.*, ASCE, 119(9), 1048-1054.

Richardson, J. E., and Panchang, V. G. (1998). "Three-dimensional simulation of scour-inducing flow at bridge piers." *J. Hydr. Engrg.*, ASCE, 124(5), 530-540.

Roulund, A., Sumer, B. M., Fredsϕe, J., and Michelsen, J. (1998). "3D mathematical modelling of scour around a circular pile in current." *Proc., 7th Int. Symp. on River Sedimentation*, Hong Kong, China, 131-137.

Ushijima, S., Shimizu, T. and Hosaka, M. (1998). "Application of computational method for local scouring to sand bed in front of power plants." *Annual J. Hydr. Engrg.*, JSCE, 42, 1009-1014 (in Japanese).

Yanmaz, A. M., and Alt1nbilek, H. D. (1991). "Study of time-dependent local scour around bridge piers." *J. Hydr. Engrg.*, ASCE, 117(10), 1247-1268.

Yoshizawa, A. (1984). "Statistical analysis of the deviation of the Reynolds stress from its eddy viscosity representation." *Phys. Fluids*, 27, 1377-1387.

APPENDIX - NOTATION

The following symbols are used in this paper:

A_1, A_2, A_3 = shape coefficients of sand grain for one-, two-, and three- dimensional geometrical properties, respectively;

B_* = constant in step length formula;

C_D = drag coefficient;

C_m = coefficient of added mass;

C_μ, C_1, C_2, C_3, $C_{\varepsilon 1}$, $C_{\varepsilon 2}$ = turbulence model constants;

d = diameter of bed material;

D = fluid drag force on sediment particle;

D_t = eddy viscosity coefficient;

$\mathbf{e_b}$ = direction of calculation for critical bed slope;

$\mathbf{f}$ = gravity vector ($\mathbf{f}=(0,0,-g)$);

f_s = probability density function of step length;

F = friction force between sediment particle and bed;

F_0 = constant in pick-up rate formula;

g = gravity acceleration;

g^{ij} = contravariant metric tensor;

G_* = coefficient of deviation between near-bed velocity vector and sediment movement direction;

J = Jacobian of transformation;

k = turbulent kinetic energy;

k_2 = constant in pick-up rate formula;

k_d = constant;

k_L = ratio between drag and lift forces;

m = constant in pick-up rate formula;

M = turbulence model parameter;

p = pressure;

$\mathbf{p}_{b1}$, $\mathbf{p}_{b2}$ = unit vectors parallel to local bed surface on $(x_1 - x_3)$ and $(x_2 - x_3)$ planes, respectively;

p_s = pick-up rate;

$\mathbf{p}_{sed(n)}$ = position vector of sediment after n th step from sediment pickup;

$\mathrm{Re}(h)$, $\mathrm{Re}(D)$ = Reynolds number estimated by using flow depth and structure length as characteristic length scale, respectively;

S = Strain Parameter;

S_d S_p = area of bed surface mesh projected onto horizontal $(x_1 - x_2)$ plan where sediment deposition and pick-up takes place, respectively;

$s_{(n)}$ = distance of sediment movement;

t = time;

x_1, x_2, x_3 = Cartesian coordinates (x_3 denotes vertical coordinate in this paper);

U^i, U_G^i = contravariant components of fluid and grid velocity, respectively;

$\mathbf{u}$ = fluid velocity vector;

u_{bi} = fluid velocity near bed (at the distance of $k_d d$ from bed);

u_i, u_{iG} = fluid and grid velocity components in Cartesian coordinates, respectively;

$u_{sed\,i}$, $\mathbf{u}_{sed}$ = magnitude and vector of sediment movement velocity, respectively;

$-\overline{u_i' u_j'}$ = Reynolds stress tensors in Cartesian coordinates;

V_d, V_p = deposition and pick-up volume of sediment, respectively;

W = submerged weight of a sediment particle;

z_b = bed elevation;

α = angle between the direction of maximum local bed slope and sediment movement direction;

β_1, β_2 = angle between $\mathbf{e_b}$ and friction force, and $\mathbf{e_b}$ and drag force, respectively;

Φ = coefficient of side bank slope;

η_0 = coefficient of variation of the lift force;

ε = turbulence dissipation rate;

θ_{b1}, θ_{b2} = angles of bed inclination in x_1 and x_2 directions, respectively;

θ_b = local bed slope angle;

$\theta_{b\max}$ = critical bed slope angle;

θ_p = angle between $\mathbf{p}_{b1}$ and $\mathbf{p}_{b2}$;

θ_r = angle of repose of bed materials;

λ = average step length;

λ_0 = constant in step length formula;

μ_k, μ_s = kinetic and static friction factor, respectively;

ξ^1, ξ^2, ξ^3 = boundary fitted coordinates;

ν = kinematic viscosity;

ρ, σ = fluid and sediment density, respectively;

σ_k σ_ε = turbulence model constants;

τ_{ij} = viscous stress tensors;

τ_*, τ_{*c} = magnitude of dimensionless tractive stress vector and its critical value, respectively;

ψ = angle between near-bed velocity vector and sediment movement direction; and

Ω = Rotation Parameter.

(Received August 28, 2001 ; revised March 1,2002)